Applied Mathematics & Information Sciences
An International Journal

http://dx.doi.org/10.12785/amis/090552

Using an Oblique Projection Operator for Highly Correlated Signal Direction-of-Arrival Estimations

*Chien-Chou Lin**

General Education Center, National Taipei University of Technology, 1 Sec. 3, Zhongxiao E. Rd. Taipei 10608, Taiwan

Received: 12 Feb. 2015, Revised: 15 May 2015, Accepted: 17 May 2015
Published online: 1 Sep. 2015

Abstract: In this paper, a high-resolution direction-of-arrival (DOA) estimation algorithm is proposed for highly correlated signals. This algorithm is divided into two stages. In Stage 1, a high-resolution method of DOA estimation using an oblique projection operator was applied to estimate the DOA of highly correlated signals. In Stage 2, because estimations obtained in highly correlated signal environments are prone to bias, a beamspace was built near the estimated angles from Stage 1 to reduce DOA bias. Next, the oblique projection operator was used on the beamspace to determine the characteristics of the signal source DOAs on a spatial spectrum for scanning and estimating the angle of arrival of signals. High-resolution estimations of DOA were thus obtained. Finally, computer simulations were performed to assess the performance and procedural accuracy of the proposed method.

Keywords: Oblique projection operator, beamspace, direction of arrival (DOA), multiple signal classification (MUSIC)

1 Introduction

Estimating the direction of arrival (DOA) of signals impinging on a sensor array is a fundamental aspect of employing array processing in various applications related to radar, sonar, communications, and astronomy. A number of high-resolution DOA methods based on subspace, such as multiple signal classification (MUSIC) and estimation of signal parameters via rotation invariance techniques (ESPRIT), have been developed [3, 4]. In normal circumstances, coherent or highly correlated signal sources created through multipath transmissions merge into a single signal source. When this occurs, the number of uncorrelated signal sources decreases and the rank of the source signal covariance matrix becomes less than the number of incident signal sources, severely impeding the performance of the algorithms and causing incorrect DOA estimations.

In an environment containing coherent or highly correlated signals, using a spatial spectrum to estimate the DOAs requires a preprocessing procedure, called decorrelation, to ensure that the rank of the source signal covariance matrix is equal to the number of signal sources. The spatial spectrum of the uncorrelated source signals can then be used for DOA estimations. Two major decorrelation preprocessing methods are currently used; the first method involves dimensionality reductions, in which the effective sensor elements of array sensors are reduced to correspond with the number of uncorrelated signal sources; an example of such method is the spatial smoothing technique [6,7]. The second method requires no dimensionality reductions and combines the decorrelation processing technique with the spatial spectrum algorithm for estimating the DOA; an example of such method is the frequency smoothing technique [8]. The methods discussed in [9,10,11,12,13,14] were used to estimate DOAs when both uncorrelated and coherent source signals coexisted in the system; the first step of DOA estimation involved using a traditional subspace method to estimate the DOAs of uncorrelated source signals. The uncorrelated source signal covariance matrix was either a Toeplitz-like matrix or a utilized oblique projection operator (OPO) [15,16], in which the covariance matrix removed the uncorrelated source signals and estimated the DOAs of the remaining coherent signals through decorrelation. By contrast, the Bartlett algorithm estimates DOAs using a traditional beamforming method. Although this method cannot be used to analyze DOA estimations when the angles of arrival of the two source signals are less than the width of the array lobes, the Bartlett algorithm is superior to the MUSIC method for estimating the DOAs of coherent

* Corresponding author e-mail: linjj@mail.ntut.edu.tw

signals [17,18]. The methods employed in [19,20,21] included the characteristics of this algorithm and rebuilt a steering matrix near the estimated DOAs angle. In addition, the original collected data were projected onto the beamspace extending from the steering vectors to build a new set of data. When the spatial spectrum and iteration algorithm were adopted, relatively higher-resolution DOA estimates were obtained, improving the performance.

In this paper, a high-resolution DOA estimation method used to determine the incident DOAs of highly correlated signals is proposed. This method is divided into two procedures: First, the signal subspace scale MUSIC (SSMUSIC) algorithm developed using the OPO [16] was used to estimate high-resolution DOAs for one set of source signals; however, the estimations were biases. Second, a steering matrix was rebuilt near the estimated DOAs angle. The original collected data were projected onto the beamspace extending from the steering vectors to build a new set of data. Next, the OPO on the beamspace was employed to characterize the DOAs of signal sources on a spatial spectrum for scanning and estimating the angle of arrival of the signals.

The remainder of this paper is arranged as follows: Section 2 briefly describes the data model. Section 3 introduces the beamspace, the OPO built on the beamspace, and the proposed algorithm, and Section 4 discusses several computer simulations conducted to verify the proposed algorithm's estimation performance. Finally, Section 5 concludes.

2 Data Model

Assume that a D number of far-field narrow band source signals impinge on a uniform linear array comprising M sensors at varying angles of arrival $\{\theta_1,\theta_2,\cdots,\theta_D\}$; the spacing constant between the two adjacent antenna components is d, which is 0.5 of the wavelength, and p highly correlated source signals exist in D. When $\mathbf{a}(\theta_i)=[a_1(\theta_i),a_2(\theta_i),\cdots,a_M(\theta_i)]^T$ is the $M\times 1$ steering vector of the angle-of-arrival θ_i, then $a_m(\theta)=\exp[-j2\pi d(m-1)\sin\theta/\beta]$, $m=1,2,\cdots,M$ is the response of the mth sensor to incident signals arriving from the direction θ , where $j=\sqrt{-1}$ and β is the wavelength of the signal carrier. Thus, the $M\times 1$ data vector of the array sensors at time t can be expressed as

$$\begin{aligned}\mathbf{x}(t)&=\sum_{i=1}^{p}\mathbf{a}(\theta_i)s_i(t)+\sum_{i=p+1}^{D}\mathbf{a}(\theta_i)s_i(t)+\mathbf{n}(t)\\&=\mathbf{A}_1(\theta)\mathbf{s}_1(t)+\mathbf{A}_2(\theta)\mathbf{s}_2(t)+\mathbf{n}(t)\\&=\mathbf{A}(\theta)\mathbf{s}(t)+\mathbf{n}(t),\end{aligned}\tag{1}$$

where $t=1,2,\cdots,N$ and N is the number of snapshots. Let $\mathbf{s}(t)=[\mathbf{s}_1(t),\mathbf{s}_2(t)]=[s_1(t),s_2(t),\cdots,s_D(t)]^T$ be the $D\times 1$ vector composed of signal amplitudes; $\mathbf{A}_1(\theta)=[\mathbf{a}(\theta_1),\mathbf{a}(\theta_2),\cdots,\mathbf{a}(\theta_p)]$ and $\mathbf{A}_2(\theta)=[\mathbf{a}(\theta_{p+1}),\mathbf{a}(\theta_2),\cdots,\mathbf{a}(\theta_D)]$, where $\mathbf{A}(\theta)=[\mathbf{A}_1(\theta),\mathbf{A}_2(\theta)]$ is the $M\times D$ steering matrix, and the superscript T is transposition. The noise $\mathbf{n}(t)$ of the array sensors is a white Gaussian process with zero mean and variance σ_n^2, uncorrelated with any of the source signals. Thus, the noise covariance matrix is the following unknown diagonal matrix:

$$\begin{aligned}\mathbf{R}_n&=E\{\mathbf{n}(t)\mathbf{n}^H(t)\}\\&=\sigma_n^2\cdot\mathbf{I}_M,\end{aligned}\tag{2}$$

where $E\{\bullet\}$ and the superscript H represent the expected value and the complex conjugate transpose, respectively, and $\mathbf{I}_M$ is the $M\times M$ identity matrix. The source signal covariance matrix is

$$\begin{aligned}\mathbf{R}_s&=\mathbf{A}(\theta)E\{\mathbf{s}(t)\mathbf{s}^H(t)\}\mathbf{A}^H(\theta)\\&=\mathbf{A}(\theta)\mathbf{S}\mathbf{A}^H(\theta),\end{aligned}\tag{3}$$

where

$$\mathbf{S}=E\{\mathbf{s}(t)\mathbf{s}^H(t)\}.\tag{4}$$

The input data vector of array sensors has the following $M\times M$ covariance matrix:

$$\begin{aligned}\mathbf{R}_x&=E\{\mathbf{x}(t)\mathbf{x}^H(t)\}\\&=\mathbf{A}(\theta)E\{\mathbf{s}(t)\mathbf{s}^H(t)\}\mathbf{A}^H(\theta)+E\{\mathbf{n}(t)\mathbf{n}^H(t)\}\\&=\mathbf{A}(\theta)\mathbf{S}\mathbf{A}^H(\theta)+\sigma_n^2\cdot\mathbf{I}_M\\&=\mathbf{R}_s+\mathbf{R}_n.\end{aligned}\tag{5}$$

The received source signal covariance matrix $\mathbf{R}_x$ can be substituted with the received limited sample mean $\widehat{\mathbf{R}}_x=(1/N)\sum_{t=1}^{N}\mathbf{x}(t)\mathbf{x}^H(t)$, where N is the number of snapshots.

The received source signal covariance matrix $\mathbf{R}_x$ is Hermitian and positive semidefinite; $\mathbf{S}$, $\mathbf{R}_s$, and $\mathbf{R}_n$ share the same characteristics as $\mathbf{R}_x$. Therefore, $\mathbf{R}_x$ can be diagonalized to produce the following equation:

$$\begin{aligned}\mathbf{R}_x&=\sum_{m=1}^{M}\lambda_m\mathbf{e}_m\mathbf{e}_m^H\\&=\sum_{m=1}^{D}\lambda_m\mathbf{e}_m\mathbf{e}_m^H+\mathbf{E}_n\Lambda_n\mathbf{E}_n^H,\end{aligned}\tag{6}$$

where$\lambda_1\geqslant\lambda_2\geqslant\cdots\geqslant\lambda_D\geqslant\lambda_{D+1}=\cdots=\lambda_M=\sigma_n^2$ is the eigenvalue of $\mathbf{R}_x$, the $\mathbf{e}_m$ table eigenvector of unit norm corresponds to λ_m, $m=1,2,\cdots,M$ and $\mathbf{E}_s=[\mathbf{e}_1,\mathbf{e}_2,\cdots,\mathbf{e}_D]$, $\mathbf{E}_n=[\mathbf{e}_{D+1},\mathbf{e}_{D+2},\cdots,\mathbf{e}_M]$. $\Lambda_n=\sigma_n^2\mathbf{I}_{M-D}$ is the eigenvalue diagonal matrix of $\mathbf{R}_n$. Each vector of the matrix $\mathbf{E}_s=[\mathbf{e}_1,\mathbf{e}_2,\cdots,\mathbf{e}_D]$ is orthogonal to that of the matrix $\mathbf{E}_n=[\mathbf{e}_{D+1},\mathbf{e}_{D+2},\cdots,\mathbf{e}_M]$. Moreover, for $m=1,2,\cdots,D$,

$$\mathbf{R}_s\mathbf{e}_m=(\lambda_m-\sigma_n^2)\mathbf{e}_m.\tag{7}$$

Equation (7) shows that $(\lambda_m-\sigma_n^2)$, $m=1,2,\cdots,D$ and 0, $m=D+1,D+2,\cdots,M$ are the eigenvalues of $\mathbf{R}_s$.

When the D source signals are uncorrelated and $M>D$, then $E\{s_i(t)s_i^H(t)\}$, $i=1,2,\cdots,D$ is the power of each source signal and $E\{s_i(t)s_k^H(t)\}=0$, $i\neq k$, and $k=1,2,\cdots,D$. Thus the rank of $\mathbf{R}_x$ is D and

$$\lambda_1-\sigma_n^2\geqslant\lambda_2-\sigma_n^2\geqslant\cdots\geqslant\lambda_D-\sigma_n^2>0.\tag{8}$$

Because $\mathbf{e}_1, \mathbf{e}_2, \cdots, \mathbf{e}_D$ are the eigenvectors of the signal subspace and $\mathbf{e}_{D+1}, \mathbf{e}_{D+2}, \cdots, \mathbf{e}_M$ are the eigenvectors of the noise subspace, $\{\mathbf{e}_1, \mathbf{e}_2, \cdots, \mathbf{e}_D\}$ and $\{\mathbf{e}_{D+1}, \mathbf{e}_{D+2}, \cdots, \mathbf{e}_M\}$ span the signal subspace and the noise subspace, respectively. Because $\{\mathbf{e}_1, \mathbf{e}_2, \cdots, \mathbf{e}_M\}$ is the orthogonal eigenvector of the unit norm of the corresponding eigenvalue $\{\lambda_1, \lambda_2, \cdots, \lambda_M\}$, $\mathbf{E}_s \perp \mathbf{E}_n$. These results indicate that by performing eigenvalue decomposition in the $\mathbf{R}_x$ space, the perpendicularly related signal subspace and noise subspace can be obtained. The orthogonal projection operators $\mathbf{P}_{\mathbf{E}_s}$ on the signal subspace and $\mathbf{P}_{\mathbf{E}_n}$ on the noise subspace are mutually orthogonal ($\mathbf{P}_{\mathbf{E}_s} \perp \mathbf{P}_{\mathbf{E}_n}$). In addition, $\mathbf{P}_{\mathbf{E}_s}$ and $\mathbf{P}_{\mathbf{E}_n}$ can be defined as

$$\mathbf{P}_{\mathbf{E}_s} = \mathbf{E}_s \mathbf{E}_s^H, \tag{9}$$

$$\mathbf{P}_{\mathbf{E}_n} = \mathbf{E}_n \mathbf{E}_n^H = \mathbf{I} - \mathbf{P}_{\mathbf{E}_s}, \tag{10}$$

Moreover, $\{\mathbf{e}_1, \mathbf{e}_2, \cdots, \mathbf{e}_D\}$ and $\{\mathbf{a}(\theta_1), \mathbf{a}(\theta_2), \cdots, \mathbf{a}(\theta_D)\}$ span the same signal subspace [3]. The MUSIC algorithm [3] estimates the DOAs of the source signals because the signal subspace and noise subspace are orthogonal.

In [16], the authors used the OPO to project the source signal onto the desired signal subspace, obtaining the source signal covariance from the source signal covariance matrix. Thus, the cost function of SSMUSIC [16] for DOA estimation is expressed as

$$\begin{aligned} J_{\text{SSMUSIC}}(\theta) &= \max_{\theta} \frac{\mathbf{a}(\theta)^H \mathbf{R}_s^+ \mathbf{a}(\theta)}{|\mathbf{a}^H(\theta) \mathbf{P}_{\mathrm{E}_n} \mathbf{a}(\theta)|} \\ &= \max_{\theta} \frac{\mathbf{a}(\theta)^H \mathbf{R}_s^+ \mathbf{a}(\theta)}{|\mathbf{a}^H(\theta) \mathrm{E}_n \mathbf{E}_n^H \mathbf{a}(\theta)|}, \end{aligned} \tag{11}$$

where $\mathbf{R}_s^+$ is a pseudoinverse matrix and $\mathbf{R}_s^+ = [\mathbf{A}(\theta)\mathbf{S}\mathbf{A}^H(\theta)]^+$. Because (11) is the function value derived from multiplying the MUSIC algorithm numerator by the source signal subspace, it is called the signal SSMUSIC. The computer simulations in [16] showed that DOA estimations of highly correlated source signals in an environment with a low signal-to-noise ratio (SNR) and small sample size produced a more favorable resolution than did MUSIC. When the correlation coefficient is less than 0.8, such method produces an excellent DOA estimation resolution.

In a highly correlated source signal environment, the MUSIC and SSMUSIC algorithms produce biased DOA estimates. To reduce the estimation biases, the OPO on the beamspace can be used to characterize the source signal DOAs on the spatial spectrum for scanning and estimating the angle of arrival of a source signal and obtain high-resolution estimations. Thus, the following algorithm is proposed.

3 Proposed Algorithm

In this paper, a high-resolution method for estimating DOAs of highly correlated source signals is proposed. The method is divided into two stages: First, the DOA estimations of a group of source signals is obtained using (11), and the source signals directions are determined. Second, a steering matrix is rebuilt near the estimated DOA angle determined in Stage 1. In addition, the original collected data are projected onto the beamspace extending from steering vectors to build a new set of data and OPOs, which are used to separate the desired source signal from the source signal subspace. The covariance of the desired source signal to be estimated is extracted from the source signals covariance matrix to characterize the DOAs of the desired source signals on the spatial spectrum. Stages 1 and 2 are detailed as follows.

Stage 1: Equation (11) is used to estimate high-resolution DOAs for the source signals $\left\{\widehat{\theta}_1, \widehat{\theta}_2, \cdots, \widehat{\theta}_D\right\}$. Next, according to [20,21], 0.5 is chosen as the resolution of the left and right sides of $\widehat{\theta}_i$ to obtain $\widehat{\theta}_{i^-}$ and $\widehat{\theta}_{i^+}$.

Stage 2: A $M \times 3D$ steering matrix is rebuilt as $\mathbf{W} = [\mathbf{a}(\widehat{\theta}_{1^-}), \mathbf{a}(\widehat{\theta}_1), \mathbf{a}(\widehat{\theta}_{1^+}), \cdots, \mathbf{a}(\widehat{\theta}_{D^-}), \mathbf{a}(\widehat{\theta}_D), \mathbf{a}(\widehat{\theta}_{D^+})]$. Subsequently, the new data output is written as a $3D \times 1$ vector $\mathbf{y}(t) = \mathbf{W}^H \mathbf{x}(t)$ and

$$\begin{aligned} \mathbf{y}(t) &= \mathbf{W}^H \mathbf{x}(t) \\ &= \mathbf{W}^H \mathbf{A}(\theta) \mathbf{s}(t) + \mathbf{W}^H \mathbf{n}(t). \end{aligned} \tag{12}$$

Let $\bar{\mathbf{A}}(\theta) = \mathbf{W}^H \mathbf{A}(\theta)$ and $\overline{\mathbf{n}}(t) = \mathbf{W}^H \mathbf{n}(t)$; thus,

$$\begin{aligned} \bar{\mathbf{A}}(\theta) &= \mathbf{W}^H \mathbf{A}(\theta) \\ &= [\mathbf{W}^H \mathbf{a}(\theta_1), \mathbf{W}^H \mathbf{a}(\theta_2), \cdots, \mathbf{W}^H \mathbf{a}(\theta_D)] \\ &= [\overline{\mathbf{a}}(\theta_1), \overline{\mathbf{a}}(\theta_2), \cdots, \overline{\mathbf{a}}(\theta_D)]. \end{aligned} \tag{13}$$

$\bar{\mathbf{A}}(\theta)$ in the beamspace processing serves the same role as $\mathbf{A}(\theta)$ in elementspace processing. The symbol of $\bar{\mathbf{A}}(\theta)$ is simplified as $\bar{\mathbf{A}} = \bar{\mathbf{A}}(\theta)$. Therefore,

$$\mathbf{y}(t) = \overline{\mathbf{A}} \mathbf{s}(t) + \overline{\mathbf{n}}(t). \tag{14}$$

From (14), the covariance matrix of $\mathbf{y}(t)$ is expressed as

$$\begin{aligned} \overline{\mathbf{R}}_y &= E\{\mathbf{y}(t)\mathbf{y}^H(t)\} \\ &= \overline{\mathbf{A}} \mathbf{S} \overline{\mathbf{A}}^H + E\{\overline{\mathbf{n}}(t)\overline{\mathbf{n}}^H(t)\}. \end{aligned} \tag{15}$$

Let

$$\overline{\mathbf{R}}_s = \overline{\mathbf{A}} \mathbf{S} \overline{\mathbf{A}}^H \text{ and } \overline{\mathbf{R}}_n = E\{\overline{\mathbf{n}}(t)\overline{\mathbf{n}}^H(t)\}. \tag{16}$$

Then, (15) can be rewritten as

$$\overline{\mathbf{R}}_y = \overline{\mathbf{R}}_s + \overline{\mathbf{R}}_n. \tag{17}$$

$\overline{\mathbf{R}}_y$ undergoes eigenvalue decomposition [17,18], which can be expressed as

$$\begin{aligned} \overline{\mathbf{R}}_y &= E\{\mathbf{y}(t)\mathbf{y}^H(t)\} \\ &= \sum_{m=1}^{3D} \gamma_m \mathbf{v}_m \mathbf{v}_m^H \end{aligned} \tag{18}$$

and

$$\begin{aligned}\overline{\mathbf{R}}_y &= \sum_{m=1}^{3D} \gamma_m \mathbf{v}_m \mathbf{v}_m^H \\ &= \sum_{m=1}^{D} \gamma_m \mathbf{v}_m \mathbf{v}_m^H + \sum_{m=D+1}^{3D} \gamma_m \mathbf{v}_m \mathbf{v}_m^H \\ &= [\overline{\mathbf{E}}_s \overline{\mathbf{E}}_n] \begin{bmatrix} \overline{\Lambda}_s & 0 \\ 0 & \overline{\Lambda}_n \end{bmatrix} \begin{bmatrix} \overline{\mathbf{E}}_s^H \\ \overline{\mathbf{E}}_n^H \end{bmatrix} \\ &= \overline{\mathbf{E}}_s \overline{\Lambda}_s \overline{\mathbf{E}}_s^H + \overline{\mathbf{E}}_n \overline{\Lambda}_n \overline{\mathbf{E}}_n^H, \end{aligned} \tag{19}$$

where $\gamma_1 \geqslant \gamma_2 \geqslant \cdots \geqslant \gamma_D \geqslant \gamma_{D+1} = \cdots = \gamma_{3D} = \overline{\sigma}_n{}^2$ is the eigenvalue of $\overline{\mathbf{R}}_y$ and corresponds to the eigenvector $\mathbf{v}_m$ of γ_m , $m = 1,2,\cdots,3D$ and $\overline{\mathbf{E}}_s = [\mathbf{v}_1,\cdots,\mathbf{v}_D]$ and $\overline{\mathbf{E}}_s = [\mathbf{v}_{D+1},\cdots,\mathbf{v}_{3D}]$. In the following, $\langle \bullet \rangle$ denotes the subspaces spanned by the column vectors of a matrix. In the beamspace,$\langle \overline{\mathbf{E}}_s \rangle$ and $\langle \overline{\mathbf{A}} \rangle$ are the signal subspaces, and $\langle \overline{\mathbf{E}}_n \rangle$ is the noise subspace; the correlation between the highly correlated signals can be removed [17,18].

Next, the OPOs are established on the beamspace to project the desired source signal subspace, and the source signal is separated from highly correlated source signals. The covariance of the desired source signal is extracted from the source signals covariance matrix, thereby creating the spatial spectrum algorithm used to estimate the desired source signal DOA. To ensure that the algorithm is valid for general applications, the ith source signal was chosen as the desired source signal to be estimated. Equation (14) can be rewritten as follows:

$$\begin{aligned}\mathbf{y}(t) &= \overline{\mathbf{a}}(\theta_i) s_i(t) + \sum_{\substack{k=1 \\ k \neq i}}^{D} \overline{\mathbf{a}}(\theta_k) s_k(t) + \overline{\mathbf{n}}(t) \\ &= \overline{\mathbf{a}}(\theta_i) s_i(t) + \mathbf{B}(\theta_i)\mathbf{b}(t) + \overline{\mathbf{n}}(t). \end{aligned} \tag{20}$$

where $\mathbf{B}(\theta_i)$ is the $3D \times (3D-1)$ matrix of $\overline{\mathbf{A}}$ minus $\overline{\mathbf{a}}(\theta_i)$, and $\mathbf{b}(t)$ is the $(D-1) \times 1$ column matrix of s_i minus $\mathbf{s}(t)$. Because the signal subspace $\langle \overline{\mathbf{E}}_s \rangle$ and noise subspace $\langle \overline{\mathbf{E}}_n \rangle$ are orthogonal,$\langle \overline{\mathbf{E}}_s \rangle \oplus \langle \overline{\mathbf{E}}_n \rangle = \mathbb{C}^{3D \times 3D}$, where $\langle \overline{\mathbf{E}}_s \rangle \oplus \langle \overline{\mathbf{E}}_n \rangle$ is the direct sum of the subspaces $\langle \overline{\mathbf{E}}_s \rangle$ and $\langle \overline{\mathbf{E}}_n \rangle$. Let $\alpha_k = E\{s_k s_k^H\}$, $k = 1,2,\cdots D$; $\mathbf{S}_i$ is the $(D-1) \times (D-1)$ diagonal matrix of diagonal elements α_k, $k \neq i$. The equivalence relation for the signal covariance matrix $\overline{\mathbf{R}}_s$ [16] is obtained:

$$\overline{\mathbf{R}}_s = \begin{cases} \overline{\mathbf{R}}_y - \overline{\mathbf{E}}_n \overline{\Lambda}_n \overline{\mathbf{E}}_n^H = \overline{\mathbf{A}} \mathbf{S} \overline{\mathbf{A}}^H \\ \overline{\mathbf{a}}(\theta_i) \alpha_i \overline{\mathbf{a}}^H(\theta_i) + \mathbf{B}(\theta_i) \mathbf{S}_i \mathbf{B}^H(\theta_i) \\ \overline{\mathbf{E}}_s \overline{\Lambda}_s \overline{\mathbf{E}}_s^H. \end{cases} \tag{21}$$

The OPO $\mathbf{O}_{\overline{\mathbf{a}}(\theta_i)\mathbf{B}(\theta_i)}$ [15,16] is expressed as

$$\mathbf{O}_{\overline{\mathbf{a}}(\theta_i)\mathbf{B}(\theta_i)} = \overline{\mathbf{a}}(\theta_i)[\overline{\mathbf{a}}^H(\theta_i)\mathbf{P}^{\perp}_{\mathbf{B}(\theta_i)}\overline{\mathbf{a}}(\theta_i)]^{-1}\overline{\mathbf{a}}(\theta_i)^H \mathbf{P}^{\perp}_{\mathbf{B}(\theta_i)}. \tag{22}$$

where $\mathbf{P}^{\perp}_{\mathbf{B}(\theta_i)}$ is the orthogonal projection operator of the range space that is orthogonal to $\langle \mathbf{B}(\theta_i) \rangle$. According to (22), the range space of $\mathbf{O}_{\overline{\mathbf{a}}(\theta_i)\mathbf{B}(\theta_i)}$ is $\langle \overline{\mathbf{a}}(\theta_i) \rangle$, and the null space contains $\langle \mathbf{B}(\theta_i) \rangle$. Thus,

$$\mathbf{O}_{\overline{\mathbf{a}}(\theta_i)\mathbf{B}(\theta_i)}\, \overline{\mathbf{a}}(\theta_i) = \overline{\mathbf{a}}(\theta_i) \text{ and } \mathbf{O}_{\overline{\mathbf{a}}(\theta_i)\mathbf{B}(\theta_i)}\, \mathbf{B}(\theta_i) = 0. \tag{23}$$

$\mathbf{O}_{\overline{\mathbf{a}}(\theta_i)\mathbf{B}(\theta_i)}$ can be used to remove $\mathbf{B}(\theta)$, and $\overline{\mathbf{a}}(\theta_i)$ remains unaffected. Thus, the desired source signal to be estimated can be separated from the other source signals. The OPO $\mathbf{O}_{\overline{\mathbf{a}}(\theta_i)\mathbf{B}(\theta_i)}$ differs from the orthogonal projection operator in (9) and can only be used to remove the subspace that is orthogonal to the projected space.

To extract the desired source signal variance $E\{[\overline{\mathbf{a}}(\theta_i)s_i][\overline{\mathbf{a}}(\theta_i)s_i]^H\}$ from the source signal covariance matrix, the source signal DOA spatial spectrum estimation algorithm is developed. To obtain an accurate estimate of $[\overline{\mathbf{a}}(\theta_i)\hat{s}_i]$ of $\overline{\mathbf{a}}(\theta_i)s_i$, oblique projection is performed on $\langle \overline{\mathbf{a}}(\theta_i) \rangle$ using $\mathbf{y}(t)$; thus,

$$\begin{aligned}\overline{\mathbf{a}}(\theta_i)\hat{s}_i &= \mathbf{O}_{\overline{\mathbf{a}}(\theta_i)\mathbf{B}(\theta_i)}\mathbf{y}(t) \\ &= \overline{\mathbf{a}}(\theta_i)[\overline{\mathbf{a}}^H(\theta_i)\mathbf{P}^{\perp}_{\mathbf{B}(\theta_i)}\overline{\mathbf{a}}(\theta_i)]^{-1}\overline{\mathbf{a}}^H(\theta_i)\mathbf{P}^{\perp}_{\mathbf{B}(\theta_i)}\mathbf{y}(t). \end{aligned} \tag{24}$$

The desired source signal covariance $E\{[\overline{\mathbf{a}}(\theta_i)s_i][\overline{\mathbf{a}}(\theta_i)s_i]^H\}$ is derived from the second-order statistic $E\{[\overline{\mathbf{a}}(\theta_i)\hat{s}_i][\overline{\mathbf{a}}(\theta_i)\hat{s}_i]^H\}$ of $\overline{\mathbf{a}}(\theta_i)\hat{s}_i$. According to (23) and (24), $E\{[\overline{\mathbf{a}}(\theta_i)s_i][\overline{\mathbf{a}}(\theta_i)s_i]^H\}$ can be expressed as

$$\begin{aligned}E\{\overline{\mathbf{a}}(\theta_i)\hat{s}_i\hat{s}_i^H\overline{\mathbf{a}}^H(\theta_i)\} &= \mathbf{O}_{\overline{\mathbf{a}}(\theta_i)\mathbf{B}(\theta_i)} E\{\mathbf{y}(t)\mathbf{y}(t)^H\}\mathbf{O}^H_{\overline{\mathbf{a}}(\theta_i)\mathbf{B}(\theta_i)} \\ &= \mathbf{O}_{\overline{\mathbf{a}}(\theta_i)\mathbf{B}(\theta_i)}\overline{\mathbf{R}}_y\mathbf{O}^H_{\overline{\mathbf{a}}(\theta_i)\mathbf{B}(\theta_i)} \\ &= \overline{\mathbf{a}}(\theta_i)\alpha_i\mathbf{a}^H(\theta_i) \\ &\quad + \mathbf{O}_{\overline{\mathbf{a}}(\theta_i)\mathbf{B}(\theta_i)}\overline{\mathbf{E}}_n\overline{\Lambda}_n\overline{\mathbf{E}}_n^H\mathbf{O}^H_{\overline{\mathbf{a}}(\theta_i)\mathbf{B}(\theta_i)}. \end{aligned} \tag{25}$$

Next, (26) and (27) are derived from (21) and (25):

$$\mathbf{O}_{\overline{\mathbf{a}}(\theta_i)\mathbf{B}(\theta_i)}\overline{\mathbf{R}}_s\mathbf{O}^H_{\overline{\mathbf{a}}(\theta_i)\mathbf{B}(\theta_i)} = \overline{\mathbf{a}}(\theta_i)\alpha_i\overline{\mathbf{a}}^H(\theta_i), \tag{26}$$

$$\mathbf{O}_{\mathbf{B}(\theta_i)\overline{\mathbf{a}}(\theta_i)}\overline{\mathbf{R}}_s\mathbf{O}^H_{\mathbf{B}(\theta_i)\overline{\mathbf{a}}(\theta_i)} = \mathbf{B}(\theta_i)\mathbf{S}_i\mathbf{B}^H(\theta_i). \tag{27}$$

Equations (26) and (27) can be combined as

$$\begin{aligned}&\mathbf{O}_{\overline{\mathbf{a}}(\theta_i)\mathbf{B}(\theta_i)}\overline{\mathbf{R}}_s\mathbf{O}^H_{\overline{\mathbf{a}}(\theta_i)\mathbf{B}(\theta_i)} + \mathbf{O}_{\mathbf{B}(\theta_i)\overline{\mathbf{a}}(\theta_i)}\overline{\mathbf{R}}_s\mathbf{O}^H_{\mathbf{B}(\theta_i)\overline{\mathbf{a}}(\theta_i)} \\ &= \overline{\mathbf{a}}(\theta_i)\alpha_i\overline{\mathbf{a}}^H(\theta_i) + \mathbf{B}(\theta_i)\mathbf{S}_i\mathbf{B}^H(\theta_i) \\ &= \overline{\mathbf{R}}_s. \end{aligned} \tag{28}$$

According to (26), the OPO $\mathbf{O}_{\overline{\mathbf{a}}(\theta_i)\mathbf{B}(\theta_i)}$ can be used to extract the desired source signal covariance from $\overline{\mathbf{R}}_s$. In [14], when both uncorrelated and coherent source signals coexisted in the system, the uncorrelated source signals from the covariance matrix were separated; the MUSIC was then used to estimate the DOA of the uncorrelated source signals, and the high-resolution DOA estimation method was adopted to estimate the remaining coherent source signals, thereby improving the estimation performance and resolution.

To obtain the desired source signal covariance using (26), $\overline{\mathbf{R}}_s$ and $\mathbf{O}_{\overline{\mathbf{a}}(\theta_i)\mathbf{B}(\theta_i)}$ must be determined first. The following lemmas show that the pseudoinverse matrix of $\overline{\mathbf{R}}_s$ ($\overline{\mathbf{R}}_s^+$) can be obtained from the received limited signal samples, which can be used to estimate $\overline{\mathbf{R}}_s$ and produce $\mathbf{O}_{\overline{\mathbf{a}}(\theta_i)\mathbf{B}(\theta_i)}$[14,15,16].

Lemma 3.1 The equation for the OPO $\mathbf{O}_{\overline{\mathbf{a}}(\theta_i)\mathbf{B}(\theta_i)}$ is as follows:

$$\mathbf{O}_{\overline{\mathbf{a}}(\theta_i)\mathbf{B}(\theta_i)} = \overline{\mathbf{a}}(\theta_i)[\overline{\mathbf{a}}^H(\theta_i)\overline{\mathbf{R}}_s^+\overline{\mathbf{a}}(\theta_i)]^{-1}\overline{\mathbf{a}}^H(\theta_i)\overline{\mathbf{R}}_s^+, \quad (29)$$

and

$$\begin{aligned}\mathbf{O}_{\overline{\mathbf{a}}(\theta_i)\mathbf{B}(\theta_i)}\overline{\mathbf{R}}_s\mathbf{O}^H_{\overline{\mathbf{a}}(\theta_i)\mathbf{B}(\theta_i)} &= \overline{\mathbf{a}}(\theta_i)\alpha_i\overline{\mathbf{a}}^H(\theta_i)\\ &= \overline{\mathbf{a}}(\theta_i)[\overline{\mathbf{a}}^H(\theta_i)\overline{\mathbf{R}}_s^+\overline{\mathbf{a}}(\theta_i)]^{-1}\overline{\mathbf{a}}^H(\theta_i),\end{aligned} \quad (30)$$

where $[\overline{\mathbf{a}}^H(\theta_i)\overline{\mathbf{R}}_s^+\overline{\mathbf{a}}(\theta_i)]^{-1} = \alpha_i$. Here, $\overline{\mathbf{R}}_s^+ = (\overline{\mathbf{A}}\mathbf{S}\overline{\mathbf{A}}^H)^+ = \overline{\mathbf{E}}_s\overline{\Lambda}_s^{-2}\overline{\mathbf{E}}_s^H$ is the pseudoinverse matrix of $\overline{\mathbf{R}}_s$.

Proof. Please refer to Appendix 6.1.

According to Lemma 3.1, $\overline{\mathbf{R}}_s^+$ is obtained from the received limited signal samples to estimate $\overline{\mathbf{R}}_s$. Therefore, $\overline{\mathbf{a}}(\theta_i)$ in (29) is changed to $\overline{\mathbf{a}}(\theta)$ as the scanning steering vector to build a θ_i-related algorithm, in which $\theta \in [-90^\circ, 90^\circ]$ is scanned to estimate $\mathbf{O}_{\overline{\mathbf{a}}(\theta_i)\mathbf{B}(\theta_i)}$. Equation (29) is reordered to produce (31) and (32):

$$\mathbf{F}_{\overline{\mathbf{a}}(\theta)} = \overline{\mathbf{a}}(\theta)[\overline{\mathbf{a}}^H(\theta)\overline{\mathbf{R}}_s^+\overline{\mathbf{a}}(\theta)]^{-1}\overline{\mathbf{a}}^H(\theta)\overline{\mathbf{R}}_s^+, \quad (31)$$

$$\mathbf{G}_{\overline{\mathbf{a}}(\theta)} = \mathbf{P}_{\overline{\mathbf{A}}} - \mathbf{F}_{\overline{\mathbf{a}}(\theta)}, \quad (32)$$

where $\mathbf{P}_{\overline{\mathbf{A}}}$ is the orthogonal projection operator with the range space $\langle\overline{\mathbf{A}}\rangle$.

According to Theorem 3.2 of [16], let

$$\mathbf{H} = \mathbf{F}_{\overline{\mathbf{a}}(\theta)}\overline{\mathbf{R}}_s\mathbf{F}^H_{\overline{\mathbf{a}}(\theta)} + \mathbf{G}_{\overline{\mathbf{a}}(\theta)}\overline{\mathbf{R}}_s\mathbf{G}^H_{\overline{\mathbf{a}}(\theta)}, \quad (33)$$

$$\begin{aligned}&Trace\{\mathbf{H}\}\\ &= Trace\{\overline{\mathbf{R}}_s\} + 2\overline{\mathbf{a}}^H\mathbf{P}_{\overline{\mathbf{E}}_n}(\theta)\overline{\mathbf{a}}(\theta)/[\overline{\mathbf{a}}^H(\theta)\overline{\mathbf{R}}_s^+\overline{\mathbf{a}}(\theta)]\\ &\geqslant \mathrm{Trace}\{\overline{\mathbf{R}}_s\}\\ &= Trace\{\overline{\mathbf{R}}_s\},\ \text{when } \overline{\mathbf{a}}(\theta) = \overline{\mathbf{a}}(\theta_i),\end{aligned} \quad (34)$$

where $Trace\{\bullet\}$ denotes the trace of a matrix.

Proof. Please refer to Appendix 6.2.

According to (34), when the scanning angle θ is set at $[-90^\circ, 90^\circ]$ and $\overline{\mathbf{a}}^H(\theta)\mathbf{P}_{\overline{\mathbf{E}}_n}(\theta)\overline{\mathbf{a}}(\theta)/[\overline{\mathbf{a}}^H(\theta)\overline{\mathbf{R}}_s^+\overline{\mathbf{a}}(\theta)]$ equals zero, the spatial incidence angle of arrival of the source signal θ_i is obtained in a similar manner with (11) to build a peak in the power spectrum of the beamspace and estimate the source signal DOAs. The cost function for DOAs estimation is expressed as

$$\begin{aligned}f(\theta) &= \max_\theta \frac{\overline{\mathbf{a}}^H(\theta)\overline{\mathbf{R}}_s^+\overline{\mathbf{a}}(\theta)}{|\overline{\mathbf{a}}^H(\theta)\mathbf{P}_{\overline{\mathbf{E}}_n}\overline{\mathbf{a}}(\theta)|}\\ &= \max_\theta \frac{\mathbf{a}^H(\theta)\mathbf{W}\overline{\mathbf{R}}_s^+\mathbf{W}^H\mathbf{a}(\theta)}{|\mathbf{a}^H(\theta)\mathbf{W}\overline{\mathbf{E}}_n^H\overline{\mathbf{E}}_n\mathbf{W}^H\mathbf{a}(\theta)|}.\end{aligned} \quad (35)$$

The following flowchart shows the procedures of the two-stage algorithm:

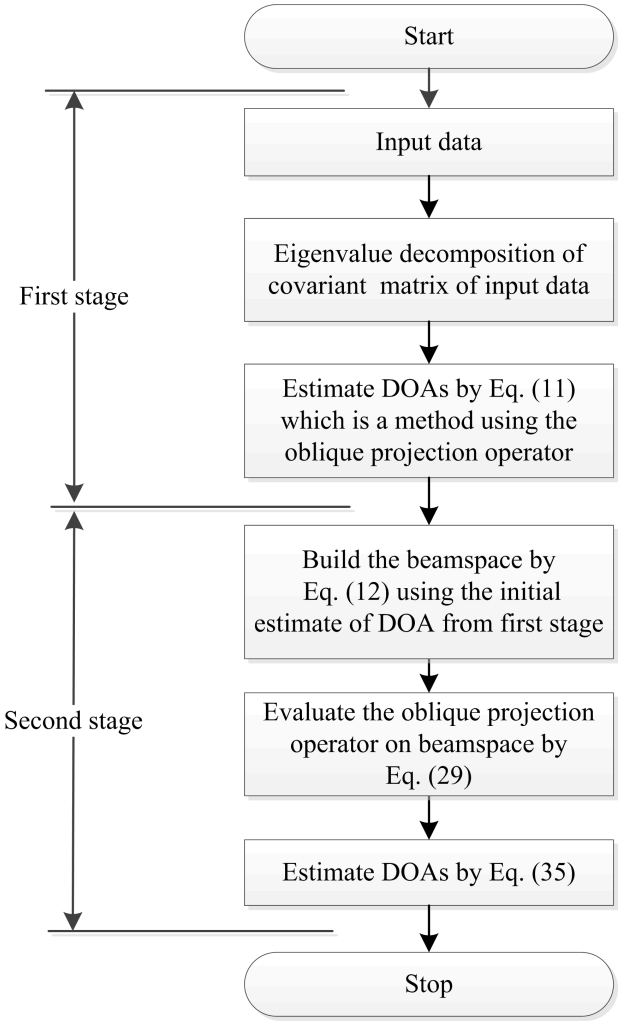

Fig. 1: Flowchart of proposed method

4 Design Examples

This section discusses computer simulations that were conducted to demonstrate the performance of DOA estimation when the proposed method was applied to uniform linear arrays. M sensor elements were located in the uniform linear arrays, and the distance between each element was half the distance of the wavelength. The SNR was the ratio between the signal power and the noise variance of each sensor element. The number of source signals was known, and the zero-mean spatially white Gaussian process was used when performing these simulations.

During the first simulation, a group of two highly correlated source signals entered the system at $\theta_1 = 0^\circ$ and $\theta_2 = 5^\circ$; the second group contained a third signal entering at $\theta_3 = 40^\circ$ and was not correlated with the aforementioned two signals. The SNR of all the source signals was 10 dB, and the number of sensor elements was $M = 8$. Fig. 2 shows that in a highly correlated source signal environment, using MUSIC in a beamspace to estimate the DOAs yielded angles of arrival the resolution of which was superior to those obtained using MUSIC in a received signal space.

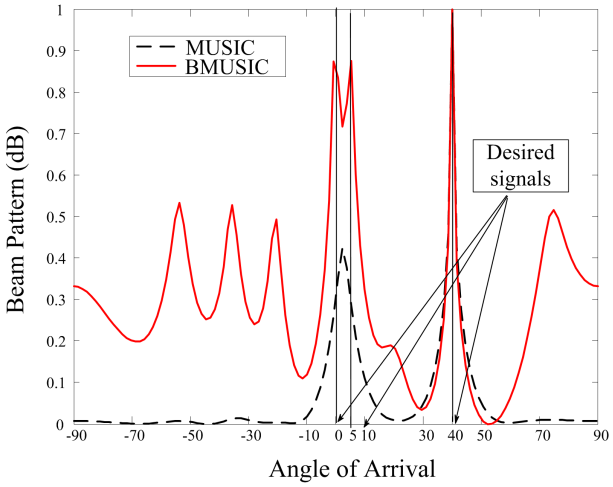

Fig. 2: Normalized spectrums of the MUSIC and MUSIC after beamspace (BMUSIC) algorithm

Conditions for the second simulation were the same those for the first; Fig. 3 depicts the $f(\theta)$ spatial spectrum. The peak of the spatial spectrum represents the angle of arrival of the source signal, and DOA estimations yielded a high resolution in highly correlated source signal environments.

The root mean square error (RMSE) was used as the performance indicator of the estimation method, and the RMSE of the DOA was expressed as

$$RMSE = \sqrt{\sum_{r=1}^{F}\sum_{i=1}^{D}(\widehat{\theta}_i(r) - \theta_i(r))^2/(FD)}, \quad (36)$$

where $\widehat{\theta}_i(r)$ is the estimate of $\theta_i(r)$ during the rth Monte Carlo test. The RMSE was used to compare the DOA estimation performance between the MUSIC, SSMUSIC [16], and proposed methods. The following simulations were obtained using 1000 Monte Carlo tests. The correlated coefficients of highly correlated source signals were defined according to [17].

For the third simulation, the performance was investigated when $M = 12$ and the SNR values differed. The experimental conditions are as follows: two highly correlated source signals with a correlated coefficient of

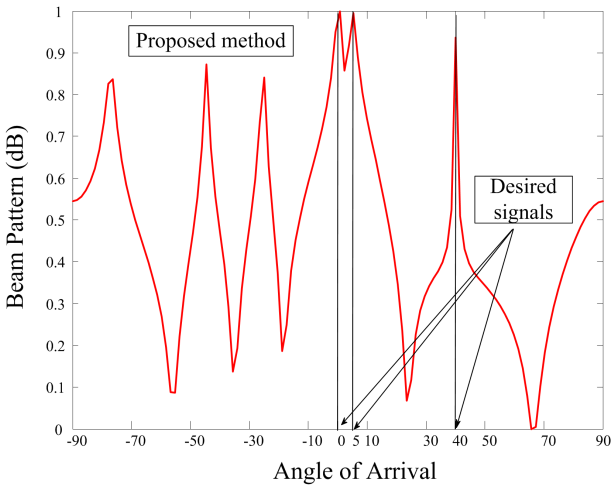

Fig. 3: Normalized spectrum of the proposed method

0.9 entered the array sensors at $\{0^\circ, 5^\circ\}$; a third uncorrelated source signal entered the array sensors at 40°; the SNR ranged from 0 dB to 20 dB; and the number of snapshots was 500. Because the received signal subspace was projected onto the beamspace to enhance the source signal characteristics, the proposed method reduced the correlation between the source signals and the estimation bias. Fig. 4 shows that the proposed method outperformed the MUSIC and SSMUSIC methods. The simulations indicate that in a low SNR environment, the SSMUSIC method outperformed the MUSIC method. However, in a high SNR environment, because the results obtained from (11) were similar to the results produced by the MUSIC method, the performance of (11) and the MUSIC method did not differ significantly. By contrast, the proposed method demonstrated an improved performance in a low SNR environment.

For the fourth simulation, the number of snapshots was varied to test the performance of the proposed method. The SNR was set at 10 dB and the number of snapshots was increased from 100 to 1000; all other conditions remained the same. The SSMUSIC method outperformed the MUSIC method in estimating DOAs when the snapshots were few. Fig. 5 shows that the proposed method outperformed the MUSIC and SSMUSIC methods when the snapshots were few; as the number of snapshots increased, the proposed method obtained excellent resolution.

For the fifth simulation, the correlated coefficients [17] were varied from 0.5 to 0.9 and the number of snapshots was set at 100; the other conditions remained the same. Fig. 6 shows that the proposed method outperformed the MUSIC and SSMUSIC methods when the snapshots were few, because the proposed method involves the beamspace for reducing the DOA estimation bias; this caused a favorable performance even when the correlated coefficients were high.

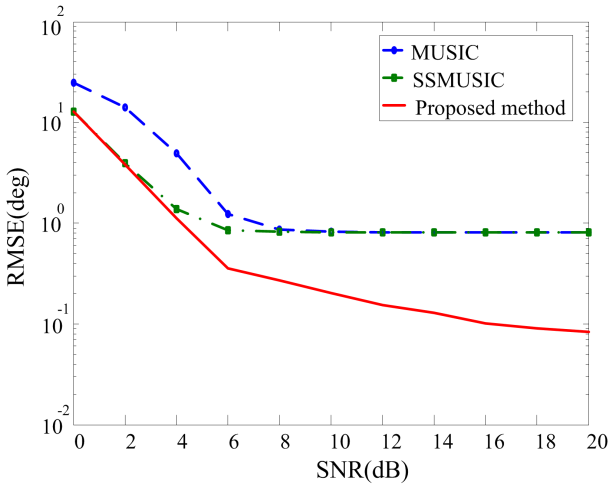

Fig. 4: RMSE of DOA estimations for varying SNRs

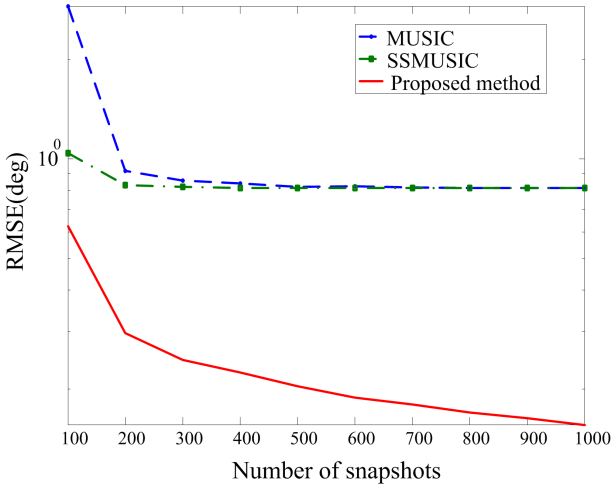

Fig. 5: RMSE of DOA estimations for a varying number of snapshots

For the last two simulations, two groups of two highly correlated source signals were used; the angles of arrival were $\{-30°, -26°\}$ and $\{0°, 5°\}$, respectively. A group of uncorrelated source signals had a 40° angle of arrival. M was set at 12 and the SNR was set at 10 dB. In the sixth simulation, the performance of the three methods was investigated by setting the correlated coefficients at 0.9 and varying the number of snapshots. Fig. 7 shows that the proposed method and the SSMUSIC method were superior to the MUSIC method [16] when the snapshots were few. As the number of snapshots increased, the proposed method outperformed the MUSIC and SSMUSIC methods. In the seventh simulation, according to the previous simulations, the number of snapshots was set at 500 and the correlated coefficients were altered from 0.5 to 0.9. Fig. 8 shows that when the correlated

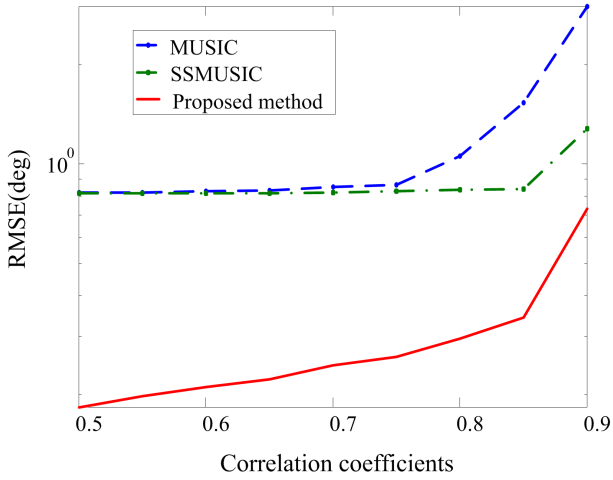

Fig. 6: RMSE of DOA estimations for varying correlation coefficients

coefficients varied, the proposed method outperformed the MUSIC and SSMUSIC methods.

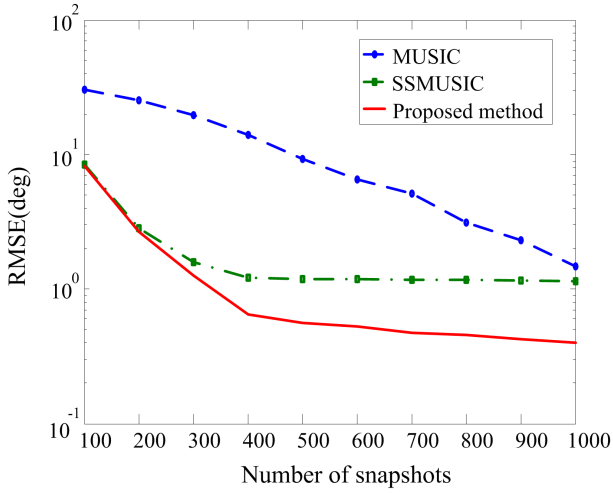

Fig. 7: RMSE of DOA estimation versus the number of snapshots.

5 Conclusion

This paper introduces a high-resolution estimation method that uses the OPO to separate desired source signals from the source signal subspace and adopts the beamspace to reduce estimation bias. Computer simulation results revealed that the proposed method yielded superior resolution in the DOA estimation results

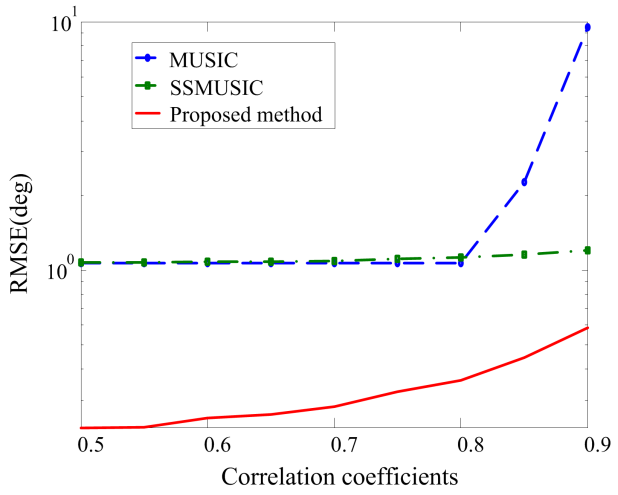

Fig. 8: RMSE of DOA estimations for varying correlation coefficients

for highly correlated signals. Moreover, the proposed method exhibited favorable DOA estimation performance when uncorrelated source signals and highly correlated source signals coexisted.

6 Appendix

According to [14,15,16], Lemma 3.1 and Theorem 3.2 were proposed. According to Lemmas 5.3h and 5.9 in [22], the pseudoinverse matrix of $\overline{\mathbf{R}}_s$ in (16) is

$$\overline{\mathbf{R}}_s^{+} = (\overline{\mathbf{A}}\mathbf{S}\overline{\mathbf{A}}^H)^{+} = (\overline{\mathbf{A}}^H)^{+}\mathbf{S}^{-1}\overline{\mathbf{A}}^{+}, \tag{37}$$

where $\overline{\mathbf{A}}^{+} = (\overline{\mathbf{A}}^H\overline{\mathbf{A}})^{-1}\overline{\mathbf{A}}^H$. Because $\overline{\mathbf{A}} = [\overline{\mathbf{a}}(\theta_i), \mathbf{B}(\theta_i)]$, the following results were obtained by using [15]:

$$\mathbf{A}^{+} = \begin{bmatrix} [\overline{\mathbf{a}}^H(\theta_i)\mathbf{P}^{\perp}_{\mathbf{B}(\theta_i)}\mathbf{a}(\theta_i)]^{-1}\overline{\mathbf{a}}^H(\theta_i)\mathbf{P}^{\perp}_{\mathbf{B}(\theta_i)} \\ [\mathbf{B}(\theta_i)\mathbf{P}^{\perp}_{\overline{\mathbf{a}}(\theta_i)}\mathbf{B}(\theta_i)]^{-1}\mathbf{B}(\theta_i)\mathbf{P}^{\perp}_{\overline{\mathbf{a}}(\theta_i)} \end{bmatrix}. \tag{38}$$

According to the definitions of the pseudoinverse matrix and orthogonal projection, the following basic characteristics were derived:

$$\overline{\mathbf{R}}_s^{+}\overline{\mathbf{R}}_s\overline{\mathbf{R}}_s^{+} = \overline{\mathbf{R}}_s^{+}, \tag{39}$$

$$\mathbf{P}_{\overline{\mathbf{A}}}\overline{\mathbf{R}}_s = \overline{\mathbf{R}}_s\mathbf{P}_{\overline{\mathbf{A}}} = \overline{\mathbf{R}}_s. \tag{40}$$

6.1 Proof of Lemma 3.1

Equations (37) and (38) were used to derive $\overline{\mathbf{a}}^H(\theta_i)\overline{\mathbf{R}}_s^{+}$ and obtain the following equation:

$$\begin{aligned}
&\overline{\mathbf{a}}^H(\theta_i)\overline{\mathbf{R}}_s^{+} \\
&= \overline{\mathbf{a}}^H(\overline{\mathbf{A}}\mathbf{S}\overline{\mathbf{A}}^H)^{+} \\
&= \overline{\mathbf{a}}^H(\theta_i)(\overline{\mathbf{A}}^H)^{+}\mathbf{S}^{-1}\overline{\mathbf{A}}^{+} \\
&= [\overline{\mathbf{A}}^{+}\overline{\mathbf{a}}(\theta_i)]^H\mathbf{S}^{-1}\overline{\mathbf{A}}^{+} \\
&= \left\{ \begin{bmatrix} [\overline{\mathbf{a}}^H(\theta_i)\mathbf{P}^{\perp}_{\mathbf{B}(\theta_i)}\overline{\mathbf{a}}(\theta_i)]^{-1}\overline{\mathbf{a}}^H(\theta_i)\mathbf{P}^{\perp}_{\mathbf{B}(\theta_i)} \\ [\mathbf{B}(\theta_i)\mathbf{P}^{\perp}_{\overline{\mathbf{a}}(\theta_i)}\mathbf{B}(\theta_i)]^{-1}\mathbf{B}(\theta_i)\mathbf{P}^{\perp}_{\overline{\mathbf{a}}(\theta_i)} \end{bmatrix}\overline{\mathbf{a}}(\theta_i) \right\}^H \\
&\quad \mathbf{S}^{-1}\overline{\mathbf{A}}^{+} \\
&= (\frac{1}{\alpha_i}, 0, \cdots, 0)\overline{\mathbf{A}}^{+} \\
&= \frac{1}{\alpha_i}[\overline{\mathbf{a}}^H(\theta_i)\mathbf{P}^{\perp}_{\mathbf{B}(\theta_i)}\overline{\mathbf{a}}(\theta_i)]^{-1}\overline{\mathbf{a}}^H(\theta_i)\mathbf{P}^{\perp}_{\mathbf{B}(\theta_i)}.
\end{aligned} \tag{41}$$

Thus,

$$\begin{aligned}
&\overline{\mathbf{a}}^H(\theta_i)\overline{\mathbf{R}}_s^{+}\overline{\mathbf{a}}(\theta_i) \\
&= \frac{1}{\alpha_i}[\overline{\mathbf{a}}^H(\theta_i)\mathbf{P}^{\perp}_{\mathbf{B}(\theta_i)}\overline{\mathbf{a}}(\theta_i)]^{-1}[\overline{\mathbf{a}}^H(\theta_i)\mathbf{P}^{\perp}_{\mathbf{B}(\theta_i)}\overline{\mathbf{a}}(\theta_i)] \\
&= \frac{1}{\alpha_i}.
\end{aligned} \tag{42}$$

When (37), (38), and (42) are used, the following is obtained:

$$\begin{aligned}
&\overline{\mathbf{a}}(\theta_i)[\overline{\mathbf{a}}^H(\theta_i)\overline{\mathbf{R}}_s^{+}\overline{\mathbf{a}}(\theta_i)]^{-1}\overline{\mathbf{a}}^H(\theta_i)\mathbf{R}_s^{+} \\
&= \overline{\mathbf{a}}(\theta_i)\alpha_i\overline{\mathbf{a}}^H(\theta_i)(\overline{\mathbf{A}}^H)^{+}\mathbf{S}^{-1}\overline{\mathbf{A}}^{+} \\
&= \overline{\mathbf{a}}(\theta_i)\alpha_i[\overline{\mathbf{A}}^{+}\overline{\mathbf{a}}(\theta_i)]^H\mathbf{S}^{-1}\overline{\mathbf{A}}^{+} \\
&= \overline{\mathbf{a}}(\theta_i)\alpha_i\left\{ \begin{bmatrix} [\overline{\mathbf{a}}^H(\theta_i)\mathbf{P}^{\perp}_{\mathbf{B}(\theta_i)}\overline{\mathbf{a}}(\theta_i)]^{-1}\overline{\mathbf{a}}^H(\theta_i)\mathbf{P}^{\perp}_{\mathbf{B}(\theta_i)} \\ [\mathbf{B}(\theta_i)\mathbf{P}^{\perp}_{\overline{\mathbf{a}}(\theta_i)}\mathbf{B}(\theta_i)]^{-1}\mathbf{B}(\theta_i)\mathbf{P}^{\perp}_{\overline{\mathbf{a}}(\theta_i)} \end{bmatrix}\overline{\mathbf{a}}(\theta_i) \right\}^H \\
&\quad \mathbf{S}^{-1}\overline{\mathbf{A}}^{+} \\
&= \overline{\mathbf{a}}(\theta_i)\alpha_i(\frac{1}{\alpha_i}, 0, \cdots, 0)\begin{bmatrix} [\overline{\mathbf{a}}^H(\theta_i)\mathbf{P}^{\perp}_{\mathbf{B}(\theta_i)}\overline{\mathbf{a}}(\theta_i)]^{-1}\overline{\mathbf{a}}^H(\theta_i)\mathbf{P}^{\perp}_{\mathbf{B}(\theta_i)} \\ [\mathbf{B}(\theta_i)\mathbf{P}^{\perp}_{\overline{\mathbf{a}}(\theta_i)}\mathbf{B}(\theta_i)]^{-1}\mathbf{B}(\theta_i)\mathbf{P}^{\perp}_{\overline{\mathbf{a}}(\theta_i)} \end{bmatrix} \\
&= \overline{\mathbf{a}}(\theta_i)[\overline{\mathbf{a}}^H(\theta_i)\mathbf{P}^{\perp}_{\mathbf{B}(\theta_i)}\overline{\mathbf{a}}(\theta_i)]^{-1}\overline{\mathbf{a}}^H(\theta_i)\mathbf{P}^{\perp}_{\mathbf{B}(\theta_i)}.
\end{aligned} \tag{43}$$

According to the definition of $\mathbf{O}_{\overline{\mathbf{a}}(\theta_i)\mathbf{B}(\theta_i)}$ in (22) and (43), Lemma 3.1 has been validated.

6.2 Proof of Theorem 3.2

For simplicity, $\overline{\mathbf{a}}(\theta)$ is abbreviated as $\overline{\mathbf{a}}$. When Lemma 3.1 and (39) are used, the following is obtained:

$$\begin{aligned}
\mathbf{F}_{\overline{\mathbf{a}}}\overline{\mathbf{R}}_s\mathbf{F}_{\overline{\mathbf{a}}}^H &= \overline{\mathbf{a}}[\overline{\mathbf{a}}^H\overline{\mathbf{R}}_s^{+}\overline{\mathbf{a}}]^{-1}\overline{\mathbf{a}}^H\overline{\mathbf{R}}_s^{+}\overline{\mathbf{R}}_s\overline{\mathbf{R}}_s^{+}\overline{\mathbf{a}}[\overline{\mathbf{a}}^H\overline{\mathbf{R}}_s^{+}\overline{\mathbf{a}}]^{-1}\overline{\mathbf{a}}^H \\
&= \overline{\mathbf{a}}[\overline{\mathbf{a}}^H\overline{\mathbf{R}}_s^{+}\overline{\mathbf{a}}]^{-1}\overline{\mathbf{a}}^H\overline{\mathbf{R}}_s^{+}\overline{\mathbf{a}}[\overline{\mathbf{a}}^H\overline{\mathbf{R}}_s^{+}\overline{\mathbf{a}}]^{-1}\overline{\mathbf{a}}^H \\
&= \overline{\mathbf{a}}[\overline{\mathbf{a}}^H\overline{\mathbf{R}}_s^{+}\overline{\mathbf{a}}]^{-1}\overline{\mathbf{a}}^H \\
&= \frac{1}{\overline{\mathbf{a}}^H\overline{\mathbf{R}}_s^{+}\overline{\mathbf{a}}}\overline{\mathbf{a}}\overline{\mathbf{a}}^H.
\end{aligned} \tag{44}$$

When (31), (32), (39), (40), (44), and Lemma 3.1 are used,

$$\begin{aligned}
&\mathbf{F}_{\overline{\mathbf{a}}}\overline{\mathbf{R}}_s\mathbf{F}_{\overline{\mathbf{a}}}^H+\mathbf{G}_{\overline{\mathbf{a}}}\overline{\mathbf{R}}_s\mathbf{G}_{\overline{\mathbf{a}}}^H\\
&=\mathbf{F}_{\overline{\mathbf{a}}}\overline{\mathbf{R}}_s\mathbf{F}_{\overline{\mathbf{a}}}^H+(\mathbf{P}_{\overline{\mathbf{A}}}-\mathbf{F}_{\overline{\mathbf{a}}})\overline{\mathbf{R}}_s(\mathbf{P}_{\overline{\mathbf{A}}}-\mathbf{F}_{\overline{\mathbf{a}}})^H\\
&=\frac{2}{\overline{\mathbf{a}}^H\overline{\mathbf{R}}_s^+\overline{\mathbf{a}}}\overline{\mathbf{a}}\overline{\mathbf{a}}^H+\overline{\mathbf{R}}_s-\frac{1}{\overline{\mathbf{a}}^H\overline{\mathbf{R}}_s^+\overline{\mathbf{a}}}\mathbf{P}_{\overline{\mathbf{A}}}\overline{\mathbf{a}}\overline{\mathbf{a}}^H-\frac{1}{\overline{\mathbf{a}}^H\overline{\mathbf{R}}_s^+\overline{\mathbf{a}}}\overline{\mathbf{a}}\overline{\mathbf{a}}^H\mathbf{P}_{\overline{\mathbf{A}}}\\
&=\overline{\mathbf{R}}_s+\frac{1}{\overline{\mathbf{a}}^H\overline{\mathbf{R}}_s^+\overline{\mathbf{a}}}(\mathbf{I}-\mathbf{P}_{\overline{\mathbf{A}}})\overline{\mathbf{a}}\overline{\mathbf{a}}^H+\frac{1}{\overline{\mathbf{a}}^H\overline{\mathbf{R}}_s^+\overline{\mathbf{a}}}\overline{\mathbf{a}}\overline{\mathbf{a}}^H(\mathbf{I}-\mathbf{P}_{\overline{\mathbf{A}}})\\
&=\overline{\mathbf{R}}_s+\frac{1}{\overline{\mathbf{a}}^H\overline{\mathbf{R}}_s^+\overline{\mathbf{a}}}\mathbf{P}_{\overline{\mathbf{E}}_n}\overline{\mathbf{a}}\overline{\mathbf{a}}^H+\frac{1}{\overline{\mathbf{a}}^H\overline{\mathbf{R}}_s^+\overline{\mathbf{a}}}\overline{\mathbf{a}}\overline{\mathbf{a}}^H\mathbf{P}_{\overline{\mathbf{E}}_n}. \qquad (45)
\end{aligned}$$

When (45) and the basic properties of the *Trace* are used, the following is obtained:

$$\begin{aligned}
&Trace\{\mathbf{H}\}\\
&=Trace\{\overline{\mathbf{R}}_s+\frac{1}{\overline{\mathbf{a}}^H\overline{\mathbf{R}}_s\overline{\mathbf{a}}}\mathbf{P}_{\overline{\mathbf{E}}_n}\overline{\mathbf{a}}\overline{\mathbf{a}}^H+\frac{1}{\overline{\mathbf{a}}^H\overline{\mathbf{R}}_s\overline{\mathbf{a}}}\overline{\mathbf{a}}\overline{\mathbf{a}}^H\mathbf{P}_{\overline{\mathbf{E}}_n}\}\\
&=Trace\{\overline{\mathbf{R}}_s\}+\frac{2(\overline{\mathbf{a}}^H\mathbf{P}_{\overline{\mathbf{E}}_n}\overline{\mathbf{a}})}{\overline{\mathbf{a}}^H\overline{\mathbf{R}}_s\overline{\mathbf{a}}}\\
&\geqslant Trace\{\overline{\mathbf{R}}_s\}. \qquad (46)
\end{aligned}$$

When $\mathbf{P}_{\overline{\mathbf{E}}_n}\overline{\mathbf{a}}(\theta_i)=0$, (46) is valid, thereby confirming the validity of the theorem.

References

[1] J. Capon, High-resolution frequency-wavenumber spectrum analysis, Proc. IEEE, Vol. 57 (1969), 1408-1418.

[2] H. L. Van Trees, Optimum Array Processing, Part IV of Detection, Estimation, and Modulation Theory, John Wiley, New York, 2002.

[3] R. O. Schmidt, Multiple emitter location and signal parameter estimation, IEEE Trans. Antennas and Propagation, Vol. 34 (1986), 276-280.

[4] R. Roy, and T. Kailath, ESPRIT-estimation of signal parameters via rotational invariance techniques, IEEE Trans. Acoustics, Speech and Signal Processing, Vol. 32 (1989), 984-995.

[5] S. S. Haykin, Communication Systems, John Wiley & Sons, 2000.

[6] T. Shan, M. Wax, and T. Kailath, On spatial smoothing for direction of arrival estimation of coherent signals, IEEE Trans. Acoustic, Speech and Signal Processing, Vol. 33 (1985), 806-811.

[7] S. U. Pillai and B. H. Kwon, Forward/backward spatial smoothing for coherent signal identification, IEEE Trans. Acoustics, Speech and Signal Processing, Vol. 37 (1989), 8-15.

[8] H. Wang and M. Kaven, Coherent signal-subspace processing for the detection and estimation of angles of arrival of multiple wide-band sources, IEEE Trans. Signal Processing, Vol. 33 (1985), 823-831.

[9] R. Rajagopal, and P. R. Rao, Generalized algorithm for DOA estimation in a passive sonar, IEE. Proceedings-F, Vol. 140 (1993), 12-20.

[10] E. M. Al-Ardi, R. M. Shubair, and M. E. Al-Mualla, Computationally efficient high-resolution DOA estimation in multipath environment, IEE. Proceedings-F, Vol. 140 (1993), 339-340.

[11] C. Y. Qi, Y. L. Zhang, Y. S. Zhang, and Y. Han, Spatial difference smoothing for DOA estimation of coherent signals, IEEE Signal Processing Letter, Vol. 12 (2005), 800-802.

[12] Z. F. Ye and X. Xu, DOA estimation by exploiting the symmetric configuration of uniform linear array, IEEE Trans. Antennas and Propagation, Vol. 55 (2007), 3716-3720.

[13] G. Wang, J. Xin, C. Ge, N. Zheng and A. Sano, Direction estimation of uncorrelated and coherent narrowband signals with uniform linear Array, 2011 1st International Symposium on Access Spaces (ISAS), 2011.

[14] X. Xu, Z. F. Ye, and J. H. Peng, Method of direction of arrival estimation for uncorrelated, partially correlated and coherent sources, IET Microwaves, Antennas and Propagation, Vol. 1 (2007), 949-954.

[15] R. T. Behrens and L. L. Scharf, Signal processing applications of oblique projection operators, IEEE Trans. Signal Processing, Vol. 42 (1994), 1413-1424.

[16] M. L. McCloud and L. L. Scharf, A new subspace identification algorithm for high resolution DOA estimation,, IEEE Trans. Antennas and Propagation, Vol. 50 (2002), 1382-1390.

[17] S. N. Shahi, M. Emadi, and K. Sadeghi, High resolution DOA estimation in fully coherent environments, Progress in Electromagnetics Research C, Vol. 5 (2008), 135-148.

[18] X. Y. Bu, Z. H. Liu, and K. Yang, Unbiased DOA estimation for CDMA based on selfinterference cancellation, Electronics Letter, Vol. 44 (2008), 1163-1165.

[19] Chunying Fang, Haifeng Li, Lin Ma, EEG Signal Classification Using the Event-Related Coherence and Genetic Algorithm, Advances in Brain Inspired Cognitive Systems, Vol. 7888 (2013), 92-100.

[20] C. C. Lin, A high-resolution method of DOA estimation for coherent signals, Advanced Science Letters, Vol. 19 (2013), 2039-2041.

[21] Y. L. Chen and C. C. Lin, Fuzzy system for DOA estimation of coherent signals, Applied Mechanics and Materials, Vol. 427429 (2013), 575-581.

[22] J. R. Schott, Matrix Analysis for Statistics, Wiley, Hoboken, NJ, 2005.

Chien-Chou Lin is Associate Professor of General Education Center at National Taipei University of Technology, Taipei, Taiwan. He received the Ph.D. degree in mathematics from National Changhua University of Education . His research interests are: dynamical systems, optimization theory, matrix operations and in the areas of smart antenna for direction of arrival estimation.